View metadata, citation and similar papers at core.ac.uk

brought to you by CORE

provided by Heriot Watt Pure

Heriot-Watt University

Heriot-Watt University
Research Gateway

Shear instability of nanocrystalline silicon carbide during nanometric cutting

Goel, Saurav; Luo, Xichun; Reuben, Robert Lewis

Published in:
Applied Physics Letters

DOI:
10.1063/1.4726036

Publication date:
2012

Link to publication in Heriot-Watt Research Gateway

Citation for published version (APA):
Goel, S., Luo, X., & Reuben, R. L. (2012). Shear instability of nanocrystalline silicon carbide during nanometric cutting. Applied Physics Letters, 100(23), [ARTN 231902]. 10.1063/1.4726036

General rights
Copyright and moral rights for the publications made accessible in the public portal are retained by the authors and/or other copyright owners and it is a condition of accessing publications that users recognise and abide by the legal requirements associated with these rights.

If you believe that this document breaches copyright please contact us providing details, and we will remove access to the work immediately and investigate your claim.

AIP | Applied Physics Letters

Shear instability of nanocrystalline silicon carbide during nanometric cutting

Saurav Goel, Xichun Luo, and Robert L. Reuben

Citation: Applied Physics Letters **100**, 231902 (2012); doi: 10.1063/1.4726036
View online: http://dx.doi.org/10.1063/1.4726036
View Table of Contents: http://scitation.aip.org/content/aip/journal/apl/100/23?ver=pdfcov
Published by the AIP Publishing

Articles you may be interested in

Grain boundary effects on defect production and mechanical properties of irradiated nanocrystalline SiC
J. Appl. Phys. **111**, 104322 (2012); 10.1063/1.4723648

Nanometric ductile cutting characteristics of silicon wafer using single crystal diamond tools
J. Vac. Sci. Technol. B **27**, 1361 (2009); 10.1116/1.3071855

Synthesis and compression of nanocrystalline silicon carbide
J. Appl. Phys. **104**, 123516 (2008); 10.1063/1.3043846

Simultaneous enhancement of toughness, ductility, and strength of nanocrystalline ceramics at high strain-rates
Appl. Phys. Lett. **90**, 181926 (2007); 10.1063/1.2736652

Hugoniot Measurements of High Pressure Phase Stability of TitaniumSilicon Carbide (Ti3SiC2)
AIP Conf. Proc. **706**, 77 (2004); 10.1063/1.1780188

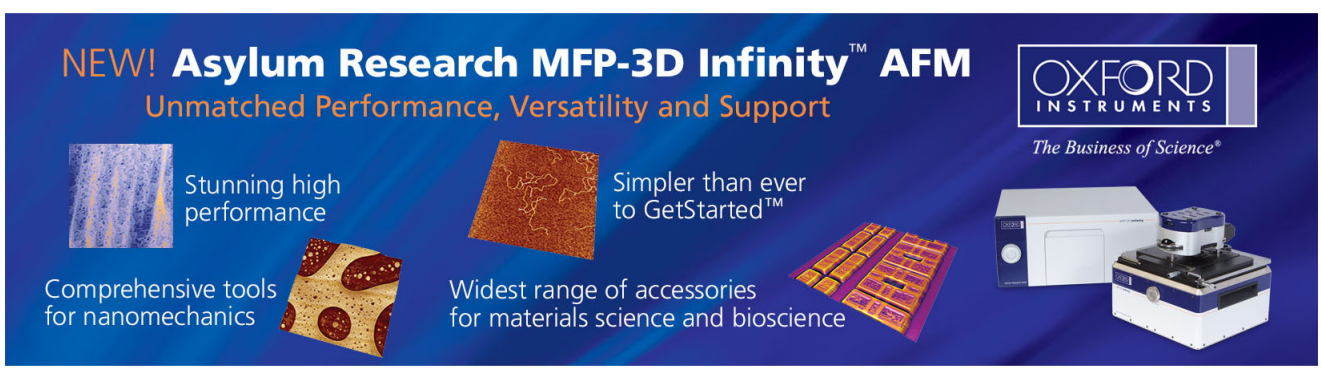

This article is copyrighted as indicated in the article. Reuse of AIP content is subject to the terms at: http://scitation.aip.org/termsconditions. Downloaded to IP: 137.195.59.30 On: Wed, 21 May 2014 15:17:58

Shear instability of nanocrystalline silicon carbide during nanometric cutting

Saurav Goel,[1] Xichun Luo,[1,2,a)] and Robert L. Reuben[1]
[1]*School of Engineering and Physical Sciences, Heriot-Watt University, Edinburgh EH144AS, United Kingdom*
[2]*School of Computing and Engineering, University of Huddersfield, Huddersfield HD13DH, United Kingdom*

(Received 17 February 2012; accepted 5 May 2012; published online 4 June 2012)

The shear instability of the nanoscrystalline 3C-SiC during nanometric cutting at a cutting speed of 100 m/s has been investigated using molecular dynamics simulation. The deviatoric stress in the cutting zone was found to cause sp^3-sp^2 disorder resulting in the local formation of SiC-graphene and Herzfeld-Mott transitions of 3C-SiC at much lower transition pressures than that required under pure compression. Besides explaining the ductility of SiC at 1500 K, this is a promising phenomenon in general nanoscale engineering of SiC. It shows that modifying the tetrahedral bonding of 3C-SiC, which would otherwise require sophisticated pressure cells, can be achieved more easily by introducing non-hydrostatic stress conditions. © *2012 American Institute of Physics*. [http://dx.doi.org/10.1063/1.4726036]

It has been widely recognized that it is the high pressure phase transformation (HPPT), now known as the Herzfeld-Mott transition[1] that causes metallization of group-IV elements such as silicon and germanium which are brittle at room temperature.[2] Such transformations are classed as metallic because they cause closure of the valence-conduction band gap due to overlap of wave functions and hence delocalization of the valence electrons.[3]

A similar phenomenon in 3C-SiC, specifically its occurrence during nanometric cutting, has yet to be investigated considering the importance of SiC as a potential candidate in large-scale quantum computing applications and high power electronic devices.[4] Earlier studies have speculated on the transformation of 3C-SiC from its original diamond cubic lattice structure to a rocksalt structure during nano-indentation and pure compression.[5,6] However, pure compression differs from hydrostatic pressure[7] as it may have a component of deviatoric stress which can cause shear induced metallization *via* changes in bond angle.[8] Also, the line contact between the cutting tip of the tool and the workpiece during nanometric cutting differs from the point contact during nano-indentation[9] so nanometric cutting conditions result in an increased energy transfer compared with nano-indentation process. If the propensity to a Herzfeld-Mott transition is a function of the nano-indentation hardness of a material,[1] the question arises as to whether or not 3C-SiC will show a rocksalt transformation or any other metallic phase during nanometric cutting. Hence, shear instability of nanocrystalline 3C-SiC during nanometric cutting became a motivational concern in the current work.

Nanometric cutting of a material using a single point diamond cutting tool is a typical practical example justifying the study of the effect of both hydrostatic and deviatoric components of stress coupled with the effect of elevated temperature. If, as suspected, the key to such processes lies in understanding the atomic level events, molecular dynamics (MD) should be an appropriate simulation approach. The relatively slow computational speed of MD can be overcome by using the multiscale simulation method which was first proposed in the year 1991.[10] Subsequently various such coupling algorithms have been proposed, a review of which has been presented by Miller and Tadmor.[11] Besides, some other coupling algorithms are also well known.[12–18] One such investigation has been recently reported by the current authors[19] involving multiscale simulation using the quasi-continuum (QC) method. However, QC is still undergoing development to simulate complex diamond cubic lattices such as 3C-SiC. Considering the above limitations, this paper adopts a state-of the-art, MD simulation employing a three-body potential energy function for describing the nanometric cutting of β-SiC (3C-SiC).

The simulation was performed using LAMMPS[20] employing a Tersoff potential energy function.[21,22] Tersoff potential energy function being three-body potential function is much better choice for covalent bond interactions of silicon and carbon in comparison to a pair potential like Morse. As a benchmark, the simulation results obtained for 3C-SiC were compared with silicon which is comparatively well studied. Both SiC and silicon were cut on the (010) surface using the cubic orientation of the diamond tool, thus maintaining the same boundary conditions. The total included angle of the diamond tool was chosen as 105° with a negative rake angle of −25° as this geometry helps to achieve better ductile response from brittle materials during nanometric cutting.[23–25] A comprehensive methodology describing the MD simulation algorithm adopted in this work has been described elsewhere.[26]

Figure 1 shows a snapshot from the MD simulation during nanometric cutting of 3C-SiC where the yellow coloured atoms represent the diamond tool, green represents silicon atoms and red represents carbon atoms from the workpiece. Figure 1 shows the chips to curl as they detach from the bulk substrate in front of the cutting tool which suggests that 3C-SiC is similar to 6H-SiC[27] in responding to the cutting forces in a ductile manner. Figure 1 also shows the region right underneath the cutting tool which experiences the highest stresses during the cutting operation. The stress representation in 3D and 2D is also shown schematically in Figure 1. The stress tensor for atom i during the simulation can be calculated using the following equation:

a)Author to whom correspondence should be addressed. Electronic mail: X.Luo@hud.ac.uk.

 © 2012 American Institute of Physics

This article is copyrighted as indicated in the article. Reuse of AIP content is subject to the terms at: http://scitation.aip.org/termsconditions. Downloaded to IP: 137.195.59.30 On: Wed, 21 May 2014 15:17:58

$$S_{ab} = -\left[\begin{array}{l} mv_a v_b + \frac{1}{2}\sum_{n=1}^{Np}(r1_a F1_b + r2_a F2_b) + \frac{1}{2}\sum_{n=1}^{Nb}(r1_a F1_b + r2_a F2_b) + \\ \frac{1}{3}\sum_{n=1}^{Na}(r1_a F1_b + r2_a F2_b + r3_a F3_b) + \frac{1}{4}\sum_{n=1}^{Nd}(r1_a F1_b + r2_a F2_b + r3_a F3_b + r4_a F4_b) \\ + \frac{1}{4}\sum_{n=1}^{Ni}(r1_a F1_b + r2_a F2_b + r3_a F3_b + r4_a F4_b) + \sum_{n=1}^{Nf} ri_a Fi_b + Kspace(r_{ia}, F_{ib}), \end{array}\right] \quad (1)$$

where a and b take on values of x,y,z to generate the 6 components of the symmetric tensor. The first term is a contribution due to the kinetic energy of atom i. The second term is a pair-wise energy contribution where n loops over the Np neighbours of atom i and $r1$ and $r2$ are the positions of the two atoms in the pair-wise interaction. $F1$ and $F2$ are the forces on the two atoms resulting from the pair-wise interactions. The third term is a bond contribution over the N_b bonds of atom i. In a similar manner, N_a angle, N_d dihedral, N_i improper interactions, and N_f internal constraints of atom i are accounted in the subsequent terms while KSpace term represent long-range Coulombic interactions.

The von Mises stress which expresses the maximum deviatoric strain energy, and governs how close the material is to yield was calculated from the components of the stress tensor (Figure 1) obtained from the simulation using Eq. (2).

$$\sigma_{von\,Mises} = \sqrt{\frac{(\sigma_{xx}-\sigma_{yy})^2 + (\sigma_{yy}-\sigma_{zz})^2 + (\sigma_{zz}-\sigma_{xx})^2 + 6(\tau_{xy}^2 + \tau_{yz}^2 + \tau_{zx}^2)}{2}}. \quad (2)$$

The maximum von Mises stress experienced by the silicon was around 12.9 GPa. A pressure of between 11 and 13 GPa[28–30] is reported to cause a phase transformation to the Si-II metallic structure, so the peak pressure during MD simulation of cutting is consistent with the polymorphic phase transformation of silicon. The magnitude of the peak von Mises stress in 3C-SiC (around 56 GPa) was found significantly higher than that of Si, suggesting higher transition pressures, if this is the cause of the peak stress. The values computed through the MD simulation are reasonably consistent with the predicted[1,31] values based on the nano-indentation hardness of materials. However, the value of transition pressure of 3C-SiC obtained in the current work was found lower than 100 GPa, which is the reported minimum pressure required to cause SiC to transform from its diamond cubic lattice to the rocksalt structure.[32] This suggests that the rocksalt structural transformation does not take place during nanometric cutting and it may not be responsible for the ductile response of 3C-SiC.

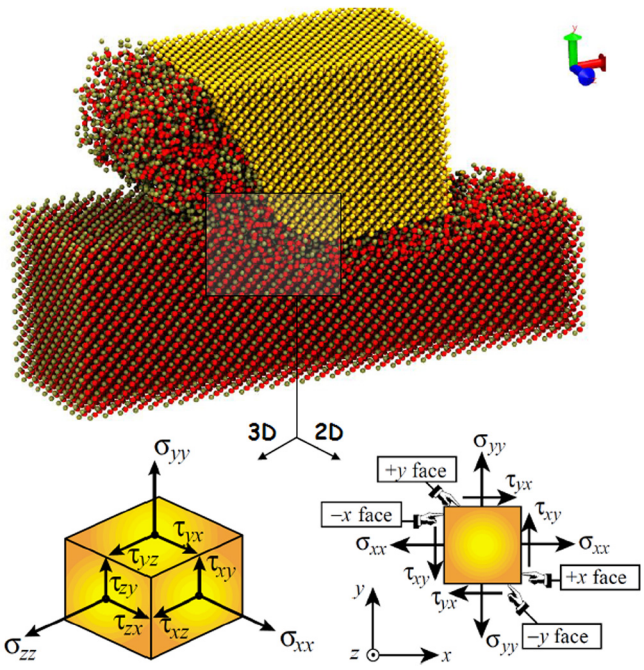

FIG. 1. Stresses in the cutting zone during machining.

Similarly, shear stress (τ_{xy}) in the workpiece for both silicon and 3C-SiC was also computed. For silicon, τ_{xy} was around 6.7 GPa while in 3C-SiC it was about 32.5 GPa. Interestingly, this magnitude of shear stress in 3C-SiC workpiece in the cutting zone was found to be of significantly higher magnitude than that exerted on a diamond grit (15 GPa) during its polishing with another diamond.[33] This observation immediately raises the question on the stability of the SiC lattice structure, since such a shear stress could certainly cause its metallization through a change in bond angle.[8] This is further consistent with the fact that SiC, in common with diamond, requires a lower force for bond-bending than bond stretching, the opposite to other typical semi-conductors such as Si, Ge, Si_3N_4, or GeAs.[34] It was therefore relevant to compute the change in bond angle during nanometric cutting in order to gain some insights. Accordingly, the bond angle distributions before and after cutting for both Si and SiC are shown in Figure 2.

It is evident from the top portion of the Figure 2 that, before nanometric cutting, there is a sharp peak in the bond angle distribution, and this is at 109.5° which corresponds to the known bond angle for both silicon and silicon carbide. However, after cutting, the bond angle distribution has

This article is copyrighted as indicated in the article. Reuse of AIP content is subject to the terms at: http://scitation.aip.org/termsconditions. Downloaded to IP: 137.195.59.30 On: Wed, 21 May 2014 15:17:58

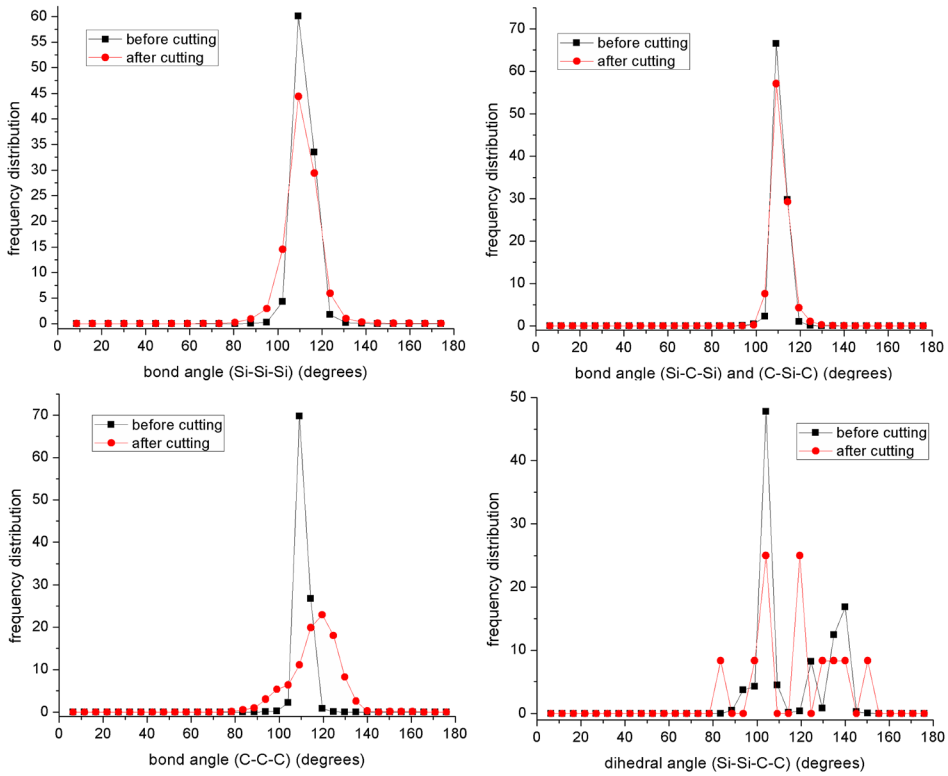

FIG. 2. Angular distribution functions of silicon and 3C-SiC.

broadened somewhat with angles for silicon appearing in the range of 80° to 140°. This wide range in bond angle is consistent with polymorphic phase transformation of silicon during nanometric cutting. By contrast, the bond angle in 3C-SiC exhibited only two values (other than 109.5°) which are 105° and 120°. This limited number of bond angles in 3C-SiC is an indication that it has not become polymorphic during nanometric cutting, unlike silicon. Additional confirmation of morphological change can be seen in the changes in C-C-C bond angle and in dihedral angle (Si-Si-C-C) brought about by the nanometric cutting. There is a distinct shift in C-C-C bond angle and Si-Si-C-C dihedral angle towards a value of 120° from the original value of 109.5°.

This change in bond angle distribution (109.5° → 120°) suggests a transformation from sp^3 to sp^2 bonding in the 3C-SiC during its nanometric cutting[35] which could be brought about by the intense shear stresses. The structure formed during this transition can be understood by the analysis of the radial distribution function (probability of finding an atom in a shell dr at a distance r from another atom chosen as a reference point), $g(r)$—shown in Figure 3.

As can be seen, there is an increase in $g(r)$ for SiC bond occurred at two interatomic distances, 1.75 Å, which is the reported length of Si=C double bonds[36] and 2.05 Å. Given the analysis of $g(r)$, bond angle and dihedral angle, suggests that the transition of sp^3-SiC to sp^2-SiC can schematically be represented as shown in top portion of Figure 4 and compared with the structure of SiC nanotube shown at bottom.

Carbon atoms are smaller than silicon atoms and are more electronegative[38] which causes the transformed structure to be chemically ordered even during its reconstruction. The geometry obtained in Figure 4 is difficult to realize through experiments,[37] however, the relevant inter-layer spacings have been obtained experimentally as 0.38 nm.[39]

This inter-layer spacing is attributed to a π-like bond and can be obtained by applying simple trigonometry to the proposed lattice structure as follows:

$$x = 2.05 \times \frac{\sin 30^\circ}{\sin 90^\circ} = 1.025 \text{ Å}$$
$$=> \text{Total inter-layer spacing} = 1.75 \text{ Å} + 2x = 3.8 \text{ Å}. \quad (3)$$

An interesting observation relevant to this phenomenon is the mechanism of cleavage on either (111) or (011) planes which is the natural shear plane during nanometric cutting. It is likely that it would have resulted in inter-plane polarization, the two surfaces having atomic charges at the extremes

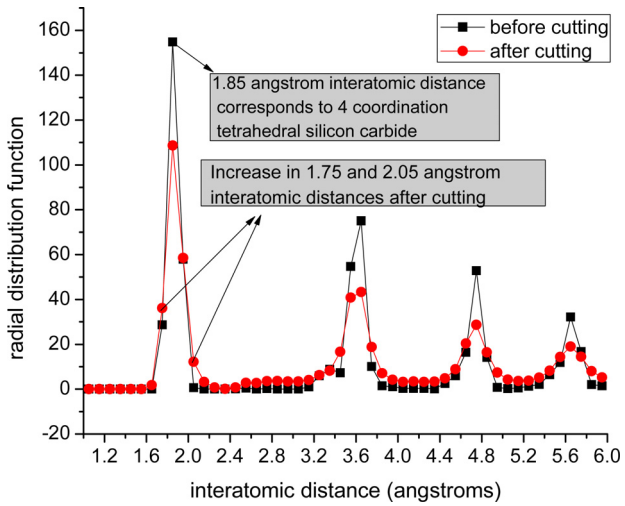

FIG. 3. Radial distribution function of 3C-SiC during nanometric cutting.

This article is copyrighted as indicated in the article. Reuse of AIP content is subject to the terms at: http://scitation.aip.org/termsconditions. Downloaded to IP: 137.195.59.30 On: Wed, 21 May 2014 15:17:58

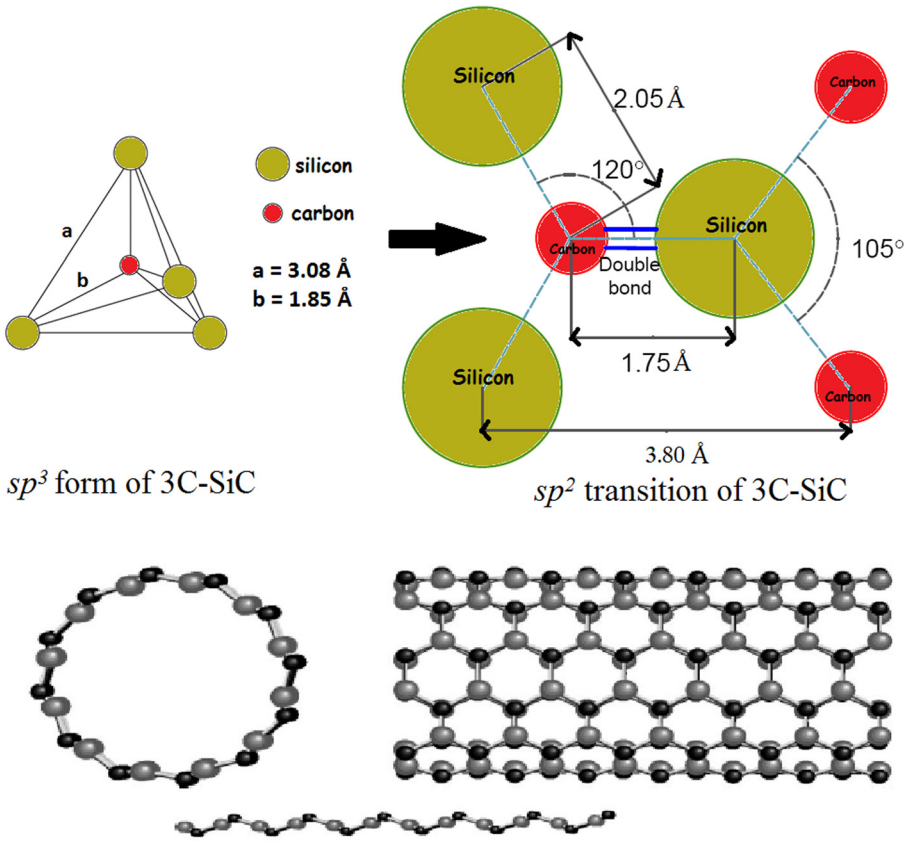

FIG. 4. sp^2 geometry of SiC from current work (top portion) and single wall SiC nanotubes with chirality (6,6 ordered) having energy 0.49 eV per SiC atomic pair and Si-C bond length between 1.79 and 1.80 Å, (bottom portion) "Reprinted with permission from Menon *et al.*, Phys. Rev. B **69**, 115322 (2004). Copyright © 2004 American Physical Society."

between silicon and carbon. The resulting structure will stabilize *via* charge transfer between the opposite diameters of silicon and carbon ($\sim 0.27|e|$[26]) or a phase transition from the wurtzite to the graphite structure.[36] It is further interesting to note that molecular stability calculations[28] have predicted the existence of a SiC graphene tube with a sp^2 structure as shown in bottom part of Figure 4.

As illustrated in the bottom panel of Figure 4, the structure is not entirely planar but is rippled with Si atoms in a single plane and C atoms in alternate rows, above and below the Si atoms. A chiral vector defined by a pair of integers (n,m) appearing in a translation vector $c = na + mb$, where a and b are the two vectors defining the primitive cell of graphene, can be used to represent such structures. The effect of this chiral vector is that the structure will be conductive, i.e., metallic, as long as n-m is a multiple of 3. It has also been suggested that the chemically ordered SiC nanotubes of "armchair" (6,6) type are slightly (by 0.05 eV/SiC atom pair) more stable than (12,0) SiC nanotubes[37] and both are conductive as n-m is multiple of 3. Further, the fact that the band gap has vanished in this form of sp^2-SiC satisfies the Herzfeld-Mott transition criterion. Hence, the sp^3-sp^2 transition in 3C-SiC is consistent with a ductile or metallic response of SiC during nanometric cutting.

Due to the unavailability of larger size single crystal 3C-SiC wafer, although an experimental trial of nanometric cutting of 3C-SiC is not possible at this stage but MD simulation suggests that the deviatoric stress during nanometric cutting brings about sp^3-sp^2 transition in 3C-SiC. The MD simulation further indicated the geometry of the sp^2 form of SiC through the analysis of radial distribution function angular distribution function and dihedral angles. Crucially, the nature of the bonding in nanocrystalline 3C-SiC can be altered by introducing non-hydrostatic stress conditions, previously thought to require much higher hydrostatic pressures.

[1]J. J. Gilman, J. Mater. Res. **7**, 535–538 (1992).
[2]J. J. Gilman, Science **261**(5127), 1436–1439 (1993).
[3]Y. Gogotsi, A. Kailer, and K. G. Nickel, J. Appl. Phys. **84**(3), 1299–1304 (1998).
[4]A. Dzurak, Nature (London) **479**(7371), 47–48 (2011).
[5]A. Noreyan, J. G. Amar, and I. Marinescu, Mater. Sci. Eng., B **117**(3), 235–240 (2005).
[6]F. Shimojo, O. Ebbsj, R. K. Kalia, A. R. Nakano, P. Jose, and P. Vashishta, Phys. Rev. Lett. **84**(15), 3338 (2000).
[7]Y. Gogotsi, A. Kailer, and K. G. Nickel, Nature (London) **401**(6754), 663–664 (1999).
[8]J. Gilman, Czech. J. Phys. **45**(11), 913–919 (1995).
[9]J. Belak, *Energy and Technology Review* (Lawrence Livermore Laboratory, 1994).
[10]S. Kohlhoff, P. Gumbsch, and H. F. Fischmeister, Philos. Mag. A **64**(4), 851–878 (1991).
[11]R. E. Miller and E. B. Tadmor, Modell. Simul. Mater. Sci. Eng. **17**(5), 053001 (2009).
[12]S. P. Xiao and T. Belytschko, Comput. Methods Appl. Mech. Eng. **193**(17–20), 1645–1669 (2004).
[13]G. J. Wagner and W. K. Liu, J. Comput. Phys. **190**(1), 249–274 (2003).
[14]P. Kerfriden, J. C. Passieux, and S. P. A. Bordas, Int. J. Numer. Methods Eng. **89**(2), 154–179 (2012).
[15]F. F. Abraham, J. Q. Broughton, N. Bernstein, and E. Kaziras, Europhys. Lett. **44**(6), 783–787 (1998).
[16]J. Q. Broughton, F. F. Abraham, N. Bernstein, and E. Kaziras Broughton, Phys. Rev. B **60**(4), 2391–2403 (1999).
[17]R. E. Rudd and J. Q. Broughton, Phys. Rev. B **58**(10), R5893–R5896 (1998).
[18]E. Saether, V. Yamakov, and E. H. Glaessgen, Int. J. Numer. Methods Eng. **78**(11), 1292–1319 (2009).
[19]H. Pen, Y. C. Liang, X. Luo, Q. Bai, S. Goel, and J. M. Ritchie, Comput. Mater. Sci. **50**(12), 3431–3441 (2011).
[20]S. Plimpton, J. Comput. Phys. **117**, 1–19 (1995).

This article is copyrighted as indicated in the article. Reuse of AIP content is subject to the terms at: http://scitation.aip.org/termsconditions. Downloaded to IP: 137.195.59.30 On: Wed, 21 May 2014 15:17:58

[21]J. Tersoff, Phys. Rev. B **39**(8), 5566 (1989).
[22]J. Tersoff, Phys. Rev. B **41**(5), 3248 (1990).
[23]R. Komanduri, Int. J. Mach. Tool Des. Res. **11**(3), 223 (1971).
[24]R. Komanduri, N. Chandrasekaran, and L. M. Raff, Wear **219**(1), 84–97 (1998).
[25]I. Durazo-Cardenas, P. Shore, X. Luo, T. Jacklin, S. Impey, and A. Cox, Wear **262**(3–4), 340–349 (2007).
[26]X. Luo, S. Goel, and R. L. Reuben, "A quantitative assessment of nanometric machinability of major polytypes of single crystal silicon carbide," J. Eur. Ceram. Soc. (2012).
[27]J. Patten, W. Gao, and K. Yasuto, J. Manuf. Sci. Eng. **127**(3), 522–532 (2005).
[28]M. B. Cai, X. P. Li, and M. Rahman, Proc. Inst. Mech. Eng., Part B **221**(10), 1511–1519 (2007).
[29]R. Komanduri and L. Raff, Proc. Inst. Mech. Eng., Part B **215**(12), 1639–1672 (2001).
[30]J. Yan, J. Appl. Phys. **95**(4), 2094–2101 (2004).
[31]J. S. Tse, D. D. Klug, and F. Gao, Phys. Rev. B **73**(14), 140102 (2006).
[32]M. Yoshida, A. Onodera, M. Ueno, K. Takemura, and O. Shimomura, Phys. Rev. B **48**(14), 10587–10590 (1993).
[33]L. Pastewka, S. Moser, P. Gumbsch, and M. Moseler, Nature Mater. **10**(1), 34–38 (2011).
[34]K. Karch, P. Pavone, W. Windl, O. Schütt, and D. Strauch, Phys. Rev. B **50**(23), 17054–17063 (1994).
[35]S. Goel, X. Luo, R. L. Reuben, and W. B. Rashid, Nanoscale Res. Lett. **6**(1), 589 (2011).
[36]P. Melinon, B. Masenelli, F. Tournus, and A. Perez, Nature Mater. **6**(7), 479–490 (2007).
[37]M. Menon, E. Richter, A. Mavrandonakis, G. Froudakis, and A. N. Andriotis, Phys. Rev. B **69**(11), 115322 (2004).
[38]A. L. Allred and E. G. Rochow, J. Inorg. Nucl. Chem. **5**(4), 269–288 (1958).
[39]X. H. Sun, C.-P. Li, W. K. Wong, N. B. Wong, C. S. Lee, S. T. Lee, and B. K. Teo, J. Am. Chem. Soc. **124**(48), 14464–14471 (2002).

This article is copyrighted as indicated in the article. Reuse of AIP content is subject to the terms at: http://scitation.aip.org/termsconditions. Downloaded to IP: 137.195.59.30 On: Wed, 21 May 2014 15:17:58